COBEM 2023 27TH INTERNATIONAL CONGRESS OF MECHANICAL ENGENEERING

ABCM Brazilian Society of Mechanical Sciences and Engineering
27th ABCM International Congress of Mechanical Engineering
December 04-08, 2023, Florianópolis-SC, Brazil

COB-2023-1728

ENERGY, EXERGY, COMBUSTION AN PERFORMANCE ASSESMENT OF A SMALL DIESEL ENGINE FUELED WITH *CRAMBE ABYSSINICA* METHYL ESTER

Omar Seye
omarseye@ufgd.edu.br
Rogério da Silva Santos
rogeriosantos@ufgd.edu.br
Ramon Eduardo Pereira Silva
Universidade Federal da Grande Dourados
Faculdade de Engenharia
Laboratório de Máquinas Térmicas, Sistemas Térmicos e Combustão
Laboratório de Energias Renováveis
Rod. Dourados-Itahum km12
Dourados MS
ramonsilva@ufgd.edu.br

Abstract. *The concerns about the increasing greenhouse effect gases emissions leads to the need of surveying environmentally friendly renewable fuels. Several studies have been carried out about the biodiesels as ethyl and methyl esters used as complementary or substitute of diesel oil in compression ignition reciprocating engines both in automotive and energetic fields. Some of these biodiesels are esterified from edible source resulting in competition with alimentation. So, the assessment of non-edible sources for compression ignitions reciprocating engines operation shows an interesting motivation. Crambe abyssinica is a non-edible oilseed present in the Cerrado biome at the Brazilian Midwest region which shows a potential opportunity to fulfill this role. This work compares the performance, energetic, exergetic and pollutant emissions of a small engine driven generator using both 100% diesel oil and 100% Crambe abyssinica Methyl Ester (CAME) as fuel. The Crambe abyssinica oil and Methyl Ester were produced at the laboratory. The grains of Crambe were cold pressed mechanically due it is the simplest and usual method for oil extraction from oilseeds. The Crambe biodiesel was produced via basic catalytic transesterification with methanol. For data collection, the generator set was instrumented to collect brake power, inlet air and fuel mass flow rates and the exhaust concentrations of the main emissions (O_2, CO_2, CO, CH_4, and NO_x). Also, the inlet airs and exhaust gas temperatures were collected. The flue gases energy rate and exergy were computed regarding the volumetric ratios of these emissions turned into mass flow rates at the measured temperatures. The inlet fuel chemical exergies were defined regarding it mass composition and the Higher Heating Values. Although the effective power delivered was lower for CAME, about 5.13%, the ester operations showed better results in efficiency parameters. Specific fuel consumption decreased by 9.58% while thermal efficiency and exergy efficiency increased by 16.94% and 17.08%, respectively. The emissions of Carbon monoxide and Unburned Hydrocarbons decreased by 8.11 % and 40.50 % respectively. The Nitrous Oxides emissions reduction remains within the gas analyzer uncertainty. These results leaded to the conclusion of its technical and environmental feasibility for compression ignition engines operation*

Keywords: *methyl-ester, compression ignition engines, energetic and exergetic, pollutant emissions, Crambe abssynica*

1. INTRODUCTION

The US Energy Information Administration (EIA) projects that global carbon dioxide (CO2) emissions from energy-related sources will continue to grow in the coming decades until 2050, in line with the increase in global energy use of about 56% from 2018 to 2050 (EIA, 2019). Among energy sources, fossil fuels supply most of the current demand of energy, about 87%, in which crude oil accounts for 33.06%, coal 30.34%, and natural gas 23.67%, respectively (Mofijur et al, 2013).

Burning of fossil fuels for power generation depends mainly on internal combustion engines, especially in the transport sector. This sector is an important component of the economy and has an impact on the development and well-being of the population. It is a sector that also contributes significantly to the amount of greenhouse gas emissions, particularly in developed and developing countries. The transport sector is responsible for 26% of global CO2 emissions and is one of the few industrial sectors where emissions are still growing (EIA, 2019)

Eventual depletion of fossil fuel reserves and its impact on the economy as well as environmental aspects associated with its use force researchers and research centers to seek alternative fuels and effective pollution control methods (Chapman, 2007; Senthil et al., 2018).

The use of biomass fuels is a technical alternative capable of minimizing these problems. Programs encouraging the production and use of biofuels have been implemented in several countries in recent decades. Some examples are ethanol in Brazil and the United States, and biodiesel, whose industrial production has been leveraged in various regions of the world in recent decades (Cordeiro et al., 2010).

The Brazilian National Agency of Petroleum, Natural Gas, and Biofuels - ANP [6] defines biodiesel as a renewable fuel obtained from a chemical process called transesterification. Through this process, triglycerides present in oils and animal fat react with a primary alcohol (methanol or ethanol), generating two products: ester and glycerin. The first can only be marketed as biodiesel after undergoing purification processes to meet quality standards, being intended mainly for application in compression ignition (diesel cycle) engines. Edible vegetable oils are among the main sources of triacylglycerols for biodiesel production (Issariyakul et al. 2008; Yin et al., 2008; Huang et al., 2010; Rashid et al., 2008).

Notwithstanding, another factor that has increased discussion on the production and use of biofuels is how it can affect food production and prices. In Brazil, the main feedstock used for ethanol production is sugarcane, which is also used in the production of sugar and starchy materials. The United States uses maize to produce ethanol, being a crop widely used to produce breakfast cereals and poultry feed. It is true that ethanol production affects the price of these materials and the costs of beef and pork products, given that maize is used to feed these animals. Therefore, the search for low-cost, nonfood energy inputs for biodiesel production has become necessary both from a technological and an economic point of view (De Oliva, 2010).

Little-known crops, such as crambe (Crambe abyssinica), emerge as an interesting alternative. Crambe is a plant native to the Mediterranean, but already adapted to Brazilian conditions. Its seeds are rich in oil and cannot be destined for human consumption due to the high erucic acid content, suggesting its use as an energy input for biodiesel production. Its oil content is approximately 40% (Bondioli,1998), consisting of more than 55% erucic acid (Bondioli,1998, Yaniv et al.,1998), rendering the oil unfit for human consumption (Lazzeri et al., 1997). The following stand out as advantages of using crambe: products with high erucic acid content have greater biodegradability in relation to its petroleum-based counterparts, being less harmful to the environment. Crambe can reach four production cycles per year and has a good yield potential: on average, 1500 kg/ha, resulting in approximately 570 kg of oil, while soybean crop has an average yield of 3000 kg/ha, resulting in 600 kg of oil (Gomes Jr, 2010; Plein et al., 2010).

The present study considers fresh crambe oil as a potential energy input for the production of an alternative fuel for an internal combustion engine. This consideration stems from the analysis of its oil content (around 40%) for biodiesel production and the fact that it is not edible. The trial engine was fueled with crambe biodiesel obtained by transesterification. Engine performance, pollutant emissions, and combustion characteristics were investigated and analyzed in comparison with diesel standards.

2. METHYL-ESTHER PRODUCTION

This section describes the *Crambe abyssinica methyl-esther (CAME) process of production.*

2.1 Crambe oil extraction

Cold Oil extraction process - The grains are cold pressed mechanically, is the simplest and usual method for oil extraction from oilseeds, consisting of a safe process without the use of organic solvents. It is basically carried out by crushing grains (in this case, crambe grains) with pressure application, partially extracting the oil and a byproduct called cake (Silva, 2017). A continuous hydraulic press (model MPE-40E) was used to extract crambe oil from oilseeds at room temperature, also obtaining the residual cake with low oil content. In this process, the grains are inserted in the press in a feed shaft, which moves them forward and compresses them. During pressing, the oil is removed at the bottom of the press, while at the other end of the feed shaft the residue called cake is removed. A sieve was used in the oil collection container so as to prevent the unpressed cake and/or crambe from contaminating the collected oil.

2.2 Transesterification and biodiesel obtention

The transesterification reaction is the step of converting the oil into methyl or ethyl esters of fatty acids, which constitute biodiesel. In this process, one mole of triglyceride reacts with three moles of alcohol (usually methanol or ethanol) in the presence of a catalyst, which can be acid or basic, forming esters (methyl or ethyl) that form biodiesel and glycerol. The transesterification reaction is reversible, requiring excess alcohol in the reaction to allow the formation of a heavier glycerol phase.

The temperature of the reaction medium can be up to 70 °C. The present study used a temperature of 25 ºC to prevent alcohol evaporation. The alkaline catalysis route is the most used because it is fast and economically viable. Other temperatures may be studied in the future to improve ester production yield (EMBRAPA,2020). The procedure for

producing biodiesel followed the steps of the flowchart in Figure 1. A previous preparation of crambe oil through a 24-hour settling was necessary to remove the dense substances accumulated in the oil that provided it with a darkened appearance. The oil drying step was also important, which consisted of heating for 30 minutes at a temperature of 105 °C, controlled by a digital thermometer.

Crambe biodiesel was produced via basic catalytic transesterification with methanol. In this study, we calculated, weighed, and crushed 15 grams of potassium hydroxide (KOH) and mixed it with 350 mL of methanol (PA-ACS) with 10-minute stirring in a magnetic stirrer at 45 °C. The methoxy solution obtained was slowly poured over 500 mL of treated crambe oil, being kept in the magnetic stirrer for 1 hour, resulting in a homogeneous mixture that was placed in a separating funnel for settling for a period of 5 days.

The reaction product generated two phases, in which the lightest phase consists of the desired ester and the heaviest (darkest) phase consists of the glycerol that was collected and disposed of properly. For the ester washing, a 0.1 N hydrochloric acid solution was used, followed by two washes with 50 ml of distilled water, each with 1 day settling. Crambe biodiesel production was completed with dehumidification to remove wastewater from the ester.

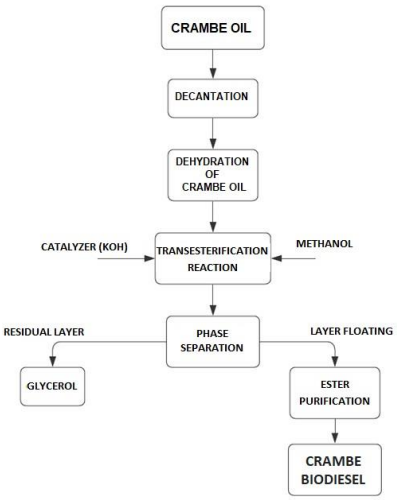

Figure 1. Flowchart of biodiesel production from crambe oil

3. THEORETICAL APPROACH

This section describes the theoretical approach of the combustion, performance, energy and exergy assessment. Also defines the control volume.

3.1 Combustion

This study used No. 2 diesel without the addition of biodiesel and without the presence of sulfur, as in Canakci & Hosoz, 2006 assuming a typical composition of $C_{14.01}H_{24.78}$, with PCI of 42.64 MJ/kg. To simplify the calculations, the authors assumed that the combustion air is dry and consists of 21% O_2 and 79% N_2 on a molar basis. As the analyzer collect the data on dry basis, the presence of water in the exhaust gases was neglected, considering that the volume fraction collected by the gas analyzer is numerically equal to the molar fraction. Our study considered NO and NO_2 formation through thermal dissociation of air N_2 and O_2, in addition to the presence of CO and unburned hydrocarbons in the form of CH_4 in the exhaust gases. The general form of the combustion equation is written in Equation (1). The reagent coefficients (from "a" to "g") are the volume (molar) fractions on a dry basis, measured by the gas sensors. The "h" coefficient was neglected. The "c" coefficient was calculated by the difference between one hundred and the sum of the other parameters.

$$\bar{N}_c.C_xH_yO_z + \bar{N}_{ar}.(O_2 + 3{,}76.N_2) \rightarrow a.CO_2 + b.CO + c.N_2 + d.O_2 + e.CH_4 + f.NO + g.N_2 + h.H_2O \qquad (1)$$

3.2 Control volume

The control volume defined in Figure 2. shows the mass ($\dot{m}$), energy ($\dot{Q}$), and exergy flows ($\dot{E}$) that cross the boundary of the control volume. Subscripts "f", "g", "l" and "d" represent, respectively: the fuel, exhaust gases, the

amount lost to the environment in the form of heat transfer, and the destroyed exergy. The brake work flow rate is represented by the electrical power ($\dot{W}_e$). The following were considered:

- The engine operates permanently.
- Intake air and exhaust gases are ideal gas mixtures.
- Volume fractions are numerically equal to molar fractions.
- The effects of the kinetic and potential energy of fluid inlet and outlet flows were neglected.
- The energy flow contained in intake air flow has been neglected as the ambient conditions are close to the standard reference state.
- The standard reference state is determined by T_0 = 298.15 and P_0 = 101.325 kPa (Mofijur et al, 2013)
- Exhaust gases leave the control volume at ambient pressure, which is close to the reference pressure.
- The energy present in the water vapor in flue gases was not considered.
- The control volume comprises the engine driven generator (EDG) as a whole.
- The measured electrical power is the mechanical power delivered by the engine.

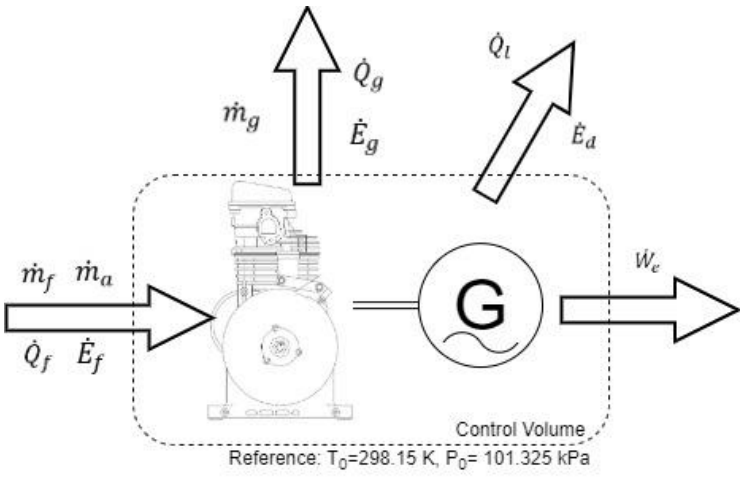

Figure 2. Mass, energy and exergy flows that cross the boundary of the control volume.

3.3 Performance parameters

Effective power, also known as brake power, is that which is effectively delivered by the engine. For this study, mechanical losses occurring in the generator are neglected. The loads are purely resistive, so the power factor is equal to 1.0. Therefore, it is assumed that the effective brake power ($\dot{W}_e$) corresponds to the electrical power measured by the wattmeter.

The brake specific fuel consumption (*bsfc*) represents the amount of fuel which is used to generate one unity of power. It is an efficiency indicatory given by the ratio between the effective brake power and the fuel mass flow ratio (Eq. (2)).

$$bsfc = \dot{m}_f / \dot{W}_e \tag{2}$$

Thermal efficiency is the ratio of the output power and input energy rate ($\dot{Q}_f$). For engine driven generators thermal efficiency can be computed by the ratio between brake power and the fuel flow energy rate (Eq. (3)). It works inversely to the bsfc; the lower the bsfc, the higher the thermal efficiency.

$$\eta_t = \dot{W}_e / \dot{Q}_f \tag{3}$$

The second law or exergetic efficiency (η_{II}) is the ratio between the output power and the exergetic fuel rate ($\dot{E}_f$) (Eq. (4)). Once thermal efficiency does not consider the effects of irreversibilities, it is expected that the exergetic efficiency presents lower values.

$$\eta_{II} = \dot{W}_e / \dot{E}_f \tag{4}$$

3.4 Energy analysis

This section shows the mathematical modeling used for energy analysis. The principles of mass and energy conservation of the first law of thermodynamics were considered. Mass flows crossing the boundary of the control volume are upstream mass air flow rate ($\dot{m}_a$) and mass fuel flow rate ($\dot{m}_f$) and exhaust gases mass flow rate ($\dot{m}_{ge}$). Mass balance is described in Equation (5).

$$\dot{m}_{ar} + \dot{m}_c = \dot{m}_g \tag{5}$$

Energy flows crossing the boundary of the control volume are upstream fuel-injected heat rate ($\dot{Q}_f$), the rate of heat present in the exhaust gases ($\dot{Q}_g$), electrical power supplied by the EDG ($\dot{W}_e$), and downstream the rate of heat lost to the environment ($\dot{Q}_l$). Energy balance is described in Equation (6).

$$\dot{Q}_f = \dot{Q}_g + \dot{Q}_l + \dot{W}_e \tag{6}$$

The heat supplied to the control volume is the product of the fuel mass flow given by combustion enthalpy, which is equal to the Lower Heating Value (LHV) of this fuel (Equation 7).

$$\dot{Q}_f = \dot{m}_f . \text{LHV} \tag{7}$$

The energy flow of flue gases is given by the product between gas flow and its specific enthalpy on a mass basis (Equation 8).

$$\dot{Q}_g = \dot{m}_g . h_g \tag{8}$$

The enthalpy of the mixture of exhaust gases on a mass basis is the ratio between the molar enthalpy ($\bar{h}_g$) and the molar mass of the MWg gases (Equation 9).

$$h_g = \bar{h}_g / MW_g \tag{9}$$

Where the specific enthalpy of exhaust gases on a molar basis is given by Equation (10).

$$\bar{h}_g = \sum_{i=1}^{j} y_i . (\bar{h}_i) \tag{10}$$

Where yi is the molar fraction of species "I" and the standard enthalpy at temperature T. The specific enthalpy of this species ($\bar{h}_i$) is determined by Equation (11) (Turns, 2011).

$$\bar{h}_i(T) = \bar{h}^0_{f,1}(T_0) + \Delta\bar{h}_{s,i}(T) \tag{11}$$

Where $\bar{h}^0_{f,1}(T_0)$ is the enthalpy of formation in the reference state (T_0 and P_0). Once the electrical power was measured in the test, the flow of the energy that is lost in the form of heat and passes through the control volume corresponds to the difference between the determined input and output rates (Equation 12).

$$\dot{Q}_l = \dot{Q}_f - (\dot{Q}_g + \dot{W}_e) \tag{12}$$

3.5 Exergy analysis

This study considered that the differences in the temperatures close to the boundary of the control volume are minimal. Thus, the authors considered that the exergy fraction corresponding to the physical am chemical exergy of the entering air can be neglected. The authors considered that the exergy fraction corresponding to the transfer of heat from the control volume to the medium is incorporated into the destroyed exergy. The determination of exergy balance followed (Canakci & Hosoz, 2006; Moran et al., 2014). The control volume and the considerations are the same used for energy balance. Exergy flows crossing the boundary of the control volume are upstream fuel exergy flow rate ($\dot{E}_f$), the rate of the exergy present in the exhaust gases ($\dot{E}_{ge}$), electrical power supplied by the EDG ($\dot{W}_{el}$), and the rate of the exergy destroyed in the form of downstream heat lost to the environment ($\dot{E}_p$). Energy balance is described in Equation (13).

$$\dot{E}_f = \dot{E}_g + \dot{E}_d + \dot{W}_e \quad (13)$$

The fuel exergy flow rate is determined by the product between fuel mass flow and its specific fuel chemical exergy (e_f^{ch}), according to Equation (14).

$$\dot{E}_f = \dot{m}_f . e_f^{ch} \quad (14)$$

The specific chemical exergy of liquid fuels can be defined on a mass basis by Equation (15) (Moran et al., 2014).

$$e_f^{ch} = [1.0401 + 0.1728. H_c + 0.0432. O_c + 0.2169. S_c . (1 - 2.0628. H_c)]. \text{LHV} \quad (15)$$

Where H_c, O_c, and S_c are the mass fractions of hydrogen, oxygen, and sulfur in relation to fuel carbon. Total exergy flow in the flue gases is given by the product between mass exhaust gases flow rate and the specific exergy of these gases (e_g) on a mass basis, according to Equation (16).

$$\dot{E}_g = \dot{m}_g . e_g \quad (16)$$

The thermomechanical exergy of flue gases, considered as a mixture of ideal gases, at temperature T and pressure P, containing n components, is obtained by Equation (17).

$$e_g^{th} = \sum_{i=1}^{j} y_i . \{h_i(T) - h_i(T_0) - T_0 . [s\,(T) - s(T_{0)}) - R . \ln\,(P/P_0)]\} \quad (17)$$

If the operating pressure is close to the reference pressure, the term $\bar{R} . \ln\,(P/P_0)$ can be neglected. Gas mixture entropy is calculated by weighting the individual enthalpies of each species (Equation 18).

$$\bar{s}_g = \sum_{i=1}^{j} y_i . (\bar{s}_i) \quad (18)$$

Individual entropies are calculated by the entropy in the standard state and by the molar fractions of each compound (Moran et al., 2014).

$$\bar{s}_i(T) = \bar{s}_i^0(T_0) - \bar{R} . ln y_i \quad (19)$$

By rearranging Equation (19), the difference between the specific entropy in the exhaust gas temperature and the reference (dead) state temperature is given by Equation (20).

$$\bar{s}_i(T) - \bar{s}_i^0(T_0) = -\bar{R} . ln y_i \quad (20)$$

Then Eq. 20 can be reduced, and thermomechanical exergy is calculated by Equation (21).

$$\bar{e}_g^{th} = \sum_{i=1}^{j} y_i . \{\bar{h}_i(T) - \bar{h}_i(T_0) - T_0 . [-\bar{R} . ln y_i\,]\} \quad (21)$$

Specific chemical exergy on a molar basis is given by Equation (22).

$$\bar{e}_g^{ch} = \sum_{i=1}^{j} y_i . \bar{e}_i^{ch} + R . T_0 . \sum_{i=1}^{j} y_i . \ln(y_i) \quad (22)$$

Analogously to the energy balance, the exergy destroyed in the control volume is the difference between the previously determined exergy entry and exit rates (Equation 23).

$$\dot{E}_d = \dot{E}_c - (\dot{E}_{ge} + \dot{W}_{el}) \quad (23)$$

The values of molar mass, enthalpy of formation, and standard chemical exergy of the exhaust gases are shown in Table 1.

Table 1. Molar mass, enthalpy of formation, and chemical exergy of flue gas components (Turns, 2011; Moran et al., 2014).

Compound	**MW [kg/kmol]**	$\bar{h}^{0}_{f,1}(T_0)$ **[kJ/kmol]**	e^{ch} **[kJ/kmol]**
Carbon Dioxide – CO2	18.016	-393547	19870
Nitrogen Dioxide – NO2	44.011	33098	55600
Methane – CH4	16.040	-74865	831650
Carbon Monoxide - CO	28.010	- 110541	275100
Nitrogen – N2	30.001	0	720
Nitric Oxide - NO	28.013	90295	88900
Oxygen – O2	31.999	0	3790

4. EXPERIMENTAL APPROACH

This section describes the experimental approach as fuel characterization, test rig, instrumentation and teste procedures.

4.1 Fuel characterization

Crambe oil is composed of six types of fatty acids: 2.18 % v/v of Palmitic (16:0), 16.49 % v/v of Oleic (18:1), 9.34 % v/v of Linoleic (18:2), 4.80% v/v of Eicosenic (20:1), and 62.5 % v/v of Euricic (22:1) (Uyaroğlu et al.,2018). The first number in parentheses shows the number of carbons in the chain, the second shows the number of double bonds in the chain. This study considered the average composition. Thereby, the composition of pure oil was $C_{20.55}H_{40,77}$, and that of Crambe Abyssinica methyl ester (CAME), considering transesterification with methanol, was $C_{21.55}H_{43.77}$.

Diesel composition, HHV, and LHV were obtained from (Canakci & Hosoz, 2006). The specific mass and kinematic viscosity for the two fuels were those published by (Uyaroğlu et al.,2018). CAME HHV was obtained in an experimental way using the heat pump IKA-C200 (using ASTM standards) and LHV was calculated considering the hydrogen content (%H) in the fuel - which will be converted into water during combustion - and the latent heat of that water. The authors considered the absence of moisture in the fuel. The values obtained and calculated are summarized in Table 2. The chemical exergy of fuels was calculated by Eq. (15).

Table 2. Physical-chemical properties of the fuels

Property	**Diesel**	**CAME**
Formulae	$C_{14.09}H_{24.78}$#	$C_{21.55}H_{40.77}O_2$
Average Molecular Weight (kg kmol-¹)	193.86	334.37
%H (m/m)	12.78%	13.18%
Higher Heating Value (kJ kg-¹)	45339#	40679
Lower Heating Value (kJ kg-¹)	42640#	40358
HC	0.91%	0.61%
OC	0.00%	0.44%
Chemical Exergy (kJ kg-¹)	44417	42026
Density @ 15 °C (kg/m³) *	840	872
Kinematic viscosity @40 °C (mm²/s) *	3.25	6.00

Canakci and Hosoz (2003)
* Uyaroğlu et al. (2018)

As shows Table 2 the difference between the calorific powers of the two fuels, as well as the amount of chemical exergy contained in a unit of fuel mass. CAME LHV was 5.35% lower than that of diesel. For the amount of chemical exergy this value rises to 5.39%. This means that there will likely be a proportional increase in fuel flow when the EDG is operating with CAME. Also, the difference between the specific masses of the two fuels. The analysis showed an increase of 3.81% for CAME in relation to diesel. However, the biggest difference occurs between kinematic viscosity values, CAME viscosity is 86.42% higher than that of diesel. Once that the fuel pump operates volumetrically and must overcome the viscous forces of the fuel, some amount of power will likely be used to supply the greatest effort of the fuel system.

4.2 Engine driven generator

The trials were performed on a motor-generator-flywheel (EDG) set (model GB3500, Gera Power Brasil®). The EDG is composed of a single-cylinder, four-stroke, air-cooled, cycle diesel engine (model ATIMA 178F), with direct injection and maximum rated power of 5.23 kW. The generator is of the alternating current type, with maximum rated power of 3.8 kVA. The technical features of the EDG are shown in Table 3.

Table 3. Main features of the EDG GB3500

Feature	Description
Type	single cylinder, air cooled, 4 strokes
Cylinder diameter	86 mm
Piston stroke	72 mm
Nominal cylinder capacity	418 cm^3
Injection	direct
Nominal rotation	3600 rpm
Maximum effective power	7.0 hp (5.22 kW)

4.3 Workbench instrumentation

For data collection, the generator set was instrumented according to the schematic drawing of the workbench shown in Figure 3

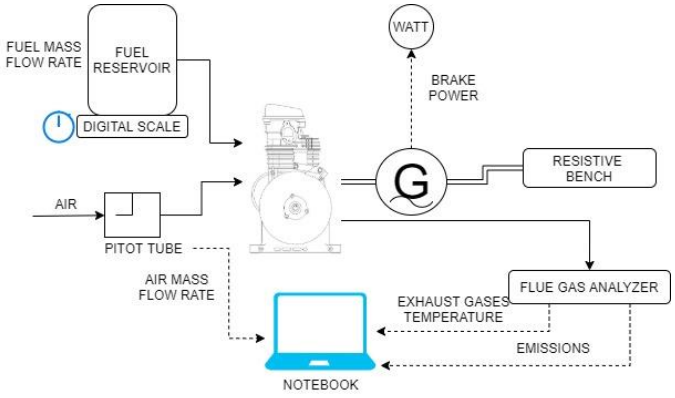

Figure 3. Details of the workbench assembly and instrumentation

The DBGas2000 program, installed on the computer, allows remote control of the equipment and continuous receipt of the data provided by the sensors. O2 and CO2 data are provided in percentage, and CO, CH4, and NOx data in parts per million (ppm). The latter must be converted into a percentage and divided by the quotient of 106. The data show the volume fraction of each component of flue gases on a dry basis. The accuracies of the instrumentation devices are shown in Table 4.

Table 4. Physical-chemical properties of the fuels

Measurement	Device	Accuracy	Unity
Mass	Digital scale	± 1.00	g
Time	Digital stopwatch	±0.01	s
Exhaust gases temperature	Type-K thermocouple	±0.10	°C
Inlet airflow	Pitot tube digital anemometer	±1.00	m^3min^{-1}

Brake power	Digital wattmeter	± 1.00	kW
O2	Eletrochemical	± 0.10	%
CO2	Nondispersive Infrared (NDIR)	± 0.30	%
CO	Eletrochemical	± 10	ppm
NOx	Eletrochemical	± 5	ppm
CH4	Nondispersive Infrared (NDIR)	± 1	ppm

4.4 Trial procedures

The authors considered a period of 1800 seconds before starting the trials so as to ensure that the engine was heated and in constant operation. For the trial, the generator set was subjected to a load of 1.40 kW. Load demand was controlled by a resistor bank. For each trial point, a period of 180 seconds was set for data collection. The electrical power delivered by the EDG was measured using a wattmeter. Because the loads are purely resistive, the power factor considered (cosφ) was 1.0. The authors assumed the absence of mechanical losses in the alternator so that its mechanical efficiency was 100%. Thus, the electrical power measured in the generator was assumed to be equal to the effective power supplied by the engine at the end of the crankshaft. Time was controlled by a digital stopwatch. Mass flow was determined gravimetrically using an auxiliary tank external to the EDG and positioned on a calibrated digital scale. Air mass flow was measured by a pitot tube anemometer, whose data were sent to the data acquisition program installed on the computer. An intake line extension was adapted to a lengthy tube so that the tip of the pitot tube was positioned more than ten diameters from the air inlet to ensure that the flow was fully developed at the measurement point. The gas analyzer probe was positioned in the exhaust. The data analysis equipment sent the volume fractions on a dry basis and the temperature of the exhaust gases to the program installed on the computer. Gas emissions and temperature data were collected at a rate of forty samples per minute, from which the arithmetic mean was used.

5. RESULTS AND DISCUSSION

The parameters of performance, consumption, exhaust temperature, and the coefficients of the combustion products already converted into a molar fraction are shown in Table 6. The data presented were compared to the theoretical approach presented previously to define the performance parameters of energy, exergy, and air pollutant emissions that will be analyzed in this section.

Table 5. Data collected.

Parameter	**Diesel**	**CAME**	**Unity**
effective brake power	1.17	1.10	kW
fuel mass flow rate	1.94 x 10-4	1.67 x 10-4	g.s-1
air mass flow rate	1.30 x 10-2	1.10 x 10-2	g.s-1
exhaust gases temperature	170.28	161.97	°C
a	0.77	0.72	%
b	8.40 x 10-5	6.98 x 10-5	%
c	79.29	79.24	%
d	19.93	20.036	%
e	1.64 x 10-5	8.80 x 10-6	%
f	6.70 x 10-5	6.14 x 10-5	%
g	1.80 x 10-5	1.50 x 10-5	%

5.1 Performance Parameters

The load demanded in the trials was 1.4 kW. Under no circumstances did the engine deliver the required load. In the operation with pure diesel oil, the effective power delivered was 1.17 kW. Therefore, in the best condition, the delivered power was 16.43% less than the demanded power. As expected, the fuel supply system consumed more of the engine power to supply the combustion chamber with CAME. The delivered power decreased by 20.71% in relation to the required power and 5.13% in relation to the delivered power when the engine operated with pure diesel oil. The decrease in power in relation to diesel oil is the result of the higher values of specific mass and viscosity of CAME in relation to diesel. Although the effective power delivered was lower for CAME, ester showed better results in efficiency parameters. Specific fuel consumption decreased by 9.58% while thermal efficiency and exergy efficiency increased by 16.94% and 17.08%, respectively. The presence of oxygen in CAME composition improves combustion efficiency, as this oxygen is more likely to be used in the combustion reaction than air oxygen. Therefore, the improvement in efficiency parameters

correlates directly with the increase in the overall efficiency of the engine. It is possible to conclude that, despite the difficulty of the engine to deliver the same power when operated with CAME or with diesel, the engine works better when operated with biodiesel. Similar results are found in Bahoosh, 2018using Sunflower oil ethyl-ester. The delivered brake power, brake specific fuel consumption, thermal efficiency and exergetic efficiency are show in Figure 4.

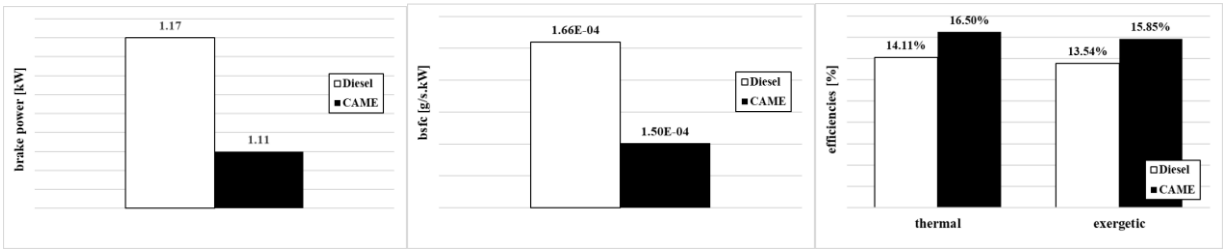

Figure 4. Brake power x demanded load, bsfc, thermal and exergetic efficiencies.

5.2 Energy and Exergy

Energy and exergy flows are shown in Figure 5. The fuel energy flow is the product of the multiplication between LHV and fuel mass flow. The mass flow of the CAME decreased by 14.61% in relation to diesel, while the difference in LHV is 5.35%. Thus, a decrease of 19.17% would be expected when the engine is operated with CAME. The actual decrease was 18.87%. The useful workflow crossing the control volume is the very definition of effective braking power already discussed in the previous discussion on performance parameters. Energy variation in the exhaust gases was 20.56% while heat loss energy varied by 21.68%. The behavior of exergy flows followed the same trend, with variations between the differences only in exhaust gas flows (19.80%) and in the exergy destroyed due to the transfer of heat to the environment (22.27%). So, using CAME led to an increase of brake thermal and exergetic efficiencies and reduction of fuel energy, fuel exergy, brake power, exhaust heat losses and destroyed exergy endorsing the study performed by (Odibi, 2019).

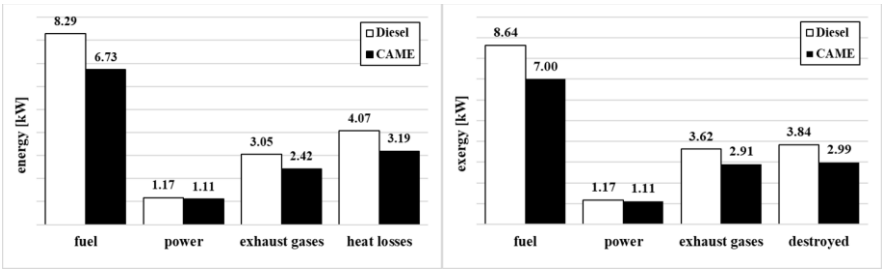

Figure 5. Energy rates and Exergy rates

The distribution of the energy supplied by the fuel to the diesel and to the CAME is shown in Figure 6. The behavior is practically the same for both fuels. Because the percentage of energy converted into power is the very definition of thermal efficiency, its values are repeated. Most of the energy supplied is lost by transfer of heat from the engine to the environment. The energy transferred by heat loss for diesel operation (49.13%) is 3.50% higher than that for CAME operation (47.47%). The difference regarding the energy contained in the exhaust gases is smaller (2.05%), with values of 36.76% for diesel and 36.02% for CAME.

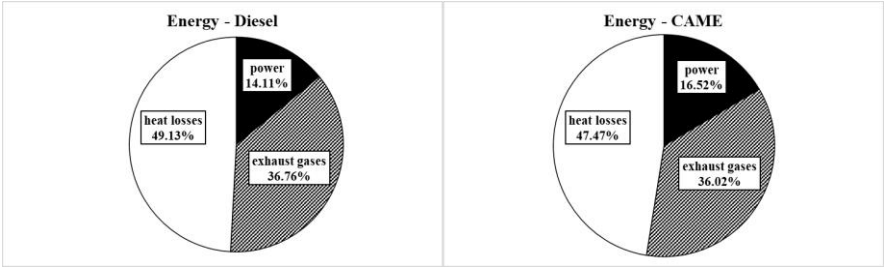

Figure 6. Energy distribution

Similarly, the distribution of the exergy supplied by the fuel is shown in Figure 7. The proportion of exergy converted into brake power corresponds to the second law efficiency. Thus, the values are the same as those of efficiency analyses already carried out. As with energy, the exergy destroyed by the transfer of heat to the environment is higher. The values of exergy destroyed for diesel and for CAME are 44.51% and 42.67%, respectively. The exergy destroyed for the two fuels with the engine operating under the same conditions was 4.31% higher for diesel. The amount of exergy destroyed is 9.40% less than the energy lost in the form of heat transfer to diesel. For CAME this difference is slightly higher (10.11%). The values of exergy contained in the exhaust gases for diesel and CAME are very close,41.94% and 41.48%, respectively, showing a difference of 4.13%. In relation to the energy available in the exhaust gases, exergy is 14.09% higher for diesel and 15.16% higher for CAME. In other words, it is in the exhaust gases that there are greater opportunities to reduce irreversibilities. This conclusion is also noticed in (Canakci & Hosoz, 2006) study which compared the energy and exergy fuel distribution in a 57-kW turbocharged diesel engine operating with diesel oil, soybean oil methyl-ester (SME) and yellow grease methyl-ester (YGME). The investigation conducted by (Çakmak and Bilgin, 2017)in a similar engine (7.3 kW, single cylinder and air cooled) to that the authors of carried out this study. Even the fuel used was a blend of 50% diesel oil and 50% corn oil methyl-ester (CME), results also corroborated with the data assessed for 100% CAME. This behavior is also confirmed by Bahoosh, 2018 and Blends et al., 2019 which carried out tests operating a 3.50 kW single-cylinder engine fueled with 8% and 15% blends of corn oil blends.

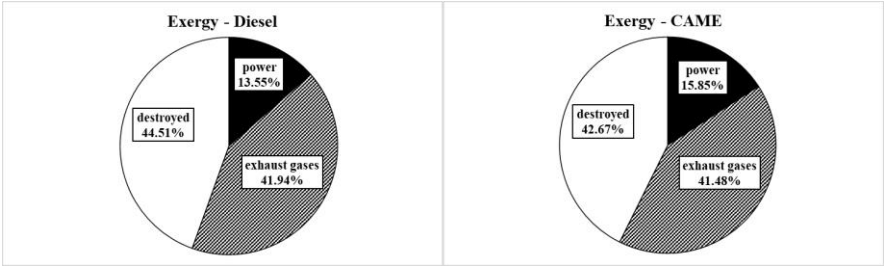

Figure 7. Exergy distribution

5.3 Pollutant emissions

Emissions resulting from incomplete combustion (CO and CH_4) and those formed due to thermal dissociation of air (NOx) were considered for the analysis. For comparison purposes the components analyzed were standardized at 20% O_2 (Carvalho Jr. and Lacava, 2003). All carbon in the fuel must be oxidized to CO_2. Carbon oxide (CO) is an intermediate product of this reaction and its presence in flue gases means that the last oxidation has not been completed. It is a toxic, odorless and colorless gas that has a density value close to that of air. Depending on concentration and exposure time it can be lethal. As oxidation is a possibility, it is a combustible gas that can still release a considerable amount of energy. Therefore, its concentration in the exhaust gases is directly proportional to combustion inefficiency. Unburned hydrocarbons (UHCs) are organic compounds that include fractions of unburned fuels or products of intermediate reactions that were not completed during the overall combustion process. In this study the UHCs are considered as methane (CH_4), which is the measurement indicated by the gas analyzer. For being the result of incomplete combustion, like CO, their presence in the exhaust gases indicates combustion inefficiency. Emissions of CO and unburned hydrocarbons (CH_4) are shown in Figure 8 The emissions of the two compounds decreased when the engine operated with CAME. For the operation with diesel oil the presence of CO is 78.92 ppm @ 20% O_2, whereas for CAME it is 75.52 ppm @ 20% O_2. These figures indicate an 8.83% decrease in CO emissions. However, this difference is much more pronounced for CH_4 emissions. The decrease is 68.06% (15.38 ppm @ 20% O_2 for diesel and 9.15 ppm @ 20% O_2 for CAME). As a conclusion, CAME operates with better combustion efficiency than diesel. This corroborates the fact that thermal, and second law efficiencies are higher for the ester. The temperature of exhaust gases reflects the behavior of the internal temperature of the cylinder; the values were 170.28 °C and 161.97 °C for diesel and CAME, respectively, corresponding to a reduction of 5.13%. The temperature in the flame zone depends on the energy available in the fuel, that is, the LHV, which is 5.35% lower for CAME. The proximity between the values of LHV reduction and exhaust temperature reflect this phenomenon. Higher temperatures improve combustion efficiency, but the results of CO and CH4 emissions show that the combustion efficiency of CAME is higher even if the internal temperature of the combustion chamber is lower. One of the processes in the burning of liquid fuels is droplet evaporation in flammable gases. In addition, the presence of oxygen in CAME composition promotes oxidant release in this process. The mixture between fuel and oxidant in the flame zone is thus facilitated, increasing combustion efficiency. However, higher temperatures induce higher NO_X formation through the thermal process of Zeldovich. When analyzing Figure 8, the difference between NO_X emissions is practically negligible despite the temperature difference. Although the presence of oxygen in CAME is beneficial for combustion efficiency, the dissociation of atmospheric air facilitates the interaction between this oxygen and the nitrogen present.

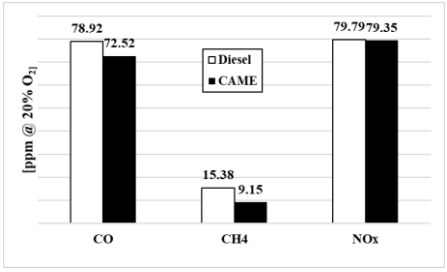

Figure 8. Carbon monoxide, unburned hydrocarbons, and nitrous oxides

6. CONCLUSIONS

This study used the first and second laws of thermodynamics to assess the performance and environmental behavior of a single-cylinder, four stroke, compression ignition engine fueled with full Crambe abyssinica methyl-ester (CAME) and compare the results to the operation with diesel. Assessing the data collected for performance, energy and exergy, and pollutant emissions, the analyses led us to the following conclusions:

1. The use of CAME resulted in higher brake thermal and exergetic efficiencies and lower fuel energy, fuel exergy, brake power, exhaust heat losses and destroyed exergy.
2. In instead of the difference of values both energy and exergy behaviors followed the same trend.
3. As CAME is an oxygenated fuel, it presented better combustion efficiency leading to lower emissions of CO and CH4. However,
4. However, CAME combustion showed a lower exhaust gases temperature value, the NOX emission values did not present considerable differences.
5. The use of CAME for compression ignition engines is both technical and environmental feasible.

7. REFERENCES

Bahoosh, R., Ghahfarokhi, M. S., Saffarian, M. R. (2018). Energy and Exergy Analysis of a Diesel Engine Running with Biodiesel Fuel. Journal of Heat and Mass Transfer Research, October, 95–104. https://doi.org/10.22075/JHMTR.2017.11293.1160

Blends, C. O., Nazzal, I. T., Rashad, R., Aldoury, J. (2019). Exergy and Energy Analysis of Diesel Engine Fuelled with Diesel and Diesel and Diesel – Corn Oil Blends. Journal of Advanced Research in Fluid Mechanics and Thermal Sciences, 63(November), 92–106.

Bondioli, P.; Folegatti, L.; Lazzeri, L.; Palmieri, S.; Native Crambe abyssinica oil and its derivatives as renewable lubricants: an approach to improve its quality by chemical and biotechnological processes; Industrial Crops and Products, 1998, 7, p 231-238.

Canakci, M., Hosoz, M. (2006). Energy and exergy analyses of a diesel engine fuelled with various biodiesels. Energy Sources, Part B: Economics, Planning and Policy, 1(4), 379–394. https://doi.org/10.1080/15567240500400796

Carvalho Jr., J. A; Lacava, P. T. Emissões em processos de combustão. (Ed. Unesp, São Paulo, 2003).

Chapman L. Transport and climate change: a review. J Transp Geogr 2007;15(5):354–67.

Cordeiro, C. S.; Ramos, L. P. Em Biodiesel in South America; Knothe, G.; Krahl, J.; Gerpen, J.V., eds.; AOCS Press: Llinois, 2010, cap. 8.3.

Çakmak A., Bilgin, A. (2017). Exergy and energy analysis with economic aspects of a diesel engine running on biodiesel-diesel fuel blends. International Jounal of Exergy, 24(January), 151–171. https://doi.org/10.1504/IJEX.2017.087700

De Oliva, A.C.E.; Qualidade de sementes de crambe submetidas a métodos de secagem e períodos de armazenamento (Dissertação de Mestrado); Universidade Estadual Paulista – UNESP, Botucatu, SP, 2010.

EMBRAPA, s.d. Ageitec: Agência Embrapa de Informação Tecnológica. [Online] Available at: https://www.agencia.cnptia.embrapa.br/gestor/agroenergia/arvore/CONT000fj0847od02wyiv802hvm3juldruvi.html [Acesso em 27 de outubro de 2020].

EIA. Energy Information Administration. International Energy Outlook; 2019 <https://www.eia.gov/outlooks/ieo/pdf/ieo2019.pdf >.

Gomes Jr, S.B.; Avaliação técnica e econômica da aplicação de óleo vegetal de crambe como isolante elétrico em comparação com óleo de soja (trabalho de conclusão de Mestrado Profissional); Instituto de Tecnologia para o Desenvolvimento – LACTEC e Insituto de Engenharia do Paraná – IEP, Curitiba, PR, 2010.

Huang, G.; Chen, F.; Wei, D.; Zhang, X.; Chen, G.; Biodiesel production by microalgal biotechnology; Applied Energy, 2010, 87, p 38–46.

Issariyakul, P.; Kulkarni, M.G.; Meher, L.C.; Dalai, A.K.; Bakhshi, N.N.; Biodiesel production from mixtures of canola oil and used cooking oil; Chemical Engineering Journal, 2008, 140, p 77–85.

Lazzeri, L.; De Mattei, F.; Bucelli, F.; Palmieri, S.; Crambe oil – a potential new hydraulic oil and quenchant; Industrial Lubrication and Tribology, 1997, 49, 2, p 71-77.

Moran M. J., Shapiro H. N., Boettner D. D., M. B. B. M. B. (2014). Fundamentals of Engineering Thermodynamics (Wiley (ed.); 8th ed.).

M. Mofijur, H.H. Masjuki, M.A. Kalam, A.E.Atabani, M.Shahabuddin, S.M. Palash, M.A.Hazrat - Effect of biodiesel from various feedstocks on combustion characteristics, engine durability and materials compatibility: A review. Renewable and Sustainable Energy Reviews 28 (2013) 441–455

Plein, G. S.; Favaro, S. P.; de Souza, A. D. V.; de Souza, C. F. T.; Ciconini, G.; dos Santos, G. P.; Miyahira, M. A. M.; Roescoe, R.; Caracterização da Fração Lipídica em Sementes de Crambe Armazenadas com e sem Casca; IV Congresso Brasileiro de Mamona e I Simpósio Internacional de Oleaginosas Energéticas, João Pessoa, PB, 2010.

Odibi, C., Babaie, M., Zare, A., Nabi, N., Bodisco, T. A., & Brown, R. J. (2019). Exergy analysis of a diesel engine with waste cooking biodiesel and triacetin. Energy Conversion and Management, 198(August), 111912. https://doi.org/10.1016/j.enconman.2019.111912

Rashid, U.; Anwar, F.; Production of biodiesel through optimized alkaline catalyzed transesterification of rapeseed oil; Fuel, 2008, 87, p 265–273.

Senthil Ramalingam, Silambarasan Rajendran, Pranesh Ganesan - Performance improvement and exhaust emissions reduction in biodiesel operated diesel engine through the use of operating parameters and catalytic converter: A review. Renewable and Sustainable Energy Reviews 81 (2018) 3215–3222.

Silva, M.M. Análise exergética da produção do biodiesel por mistura binária de sebo bovino e óleo de soja – Universidade Federal de Minas Gerais – Brasil (Master thesis) - 2017. 92 f. p.32-33

Turns, S. R. (2011). An Introduction to Combustion: Concepts and Applications (3rd ed.). McGraw-Hill Science.

Uyaroğlu, A., Uyumaz, A., & Çelikten, İ. (2018). Comparison of the combustion, performance, and emission characteristics of inedible Crambe abyssinica biodiesel and edible hazelnut, corn, soybean, sunflower, and canola biodiesels. Environmental Progress and Sustainable Energy, 37(4), 1438–1447. https://doi.org/10.1002/ep.12794

Yaniv, Z.; Shabelsky, E.; Schafferman, D.; Granot, I.; Kipnis, T.; Oil and fatty acid changes in Sinapis and Crambe seeds during germination and early development; Industrial Crops and Products, 1998, 9, p 1–8

Yin, J.Z.; Xiao, M.; Wang, A.Q.; Xiu, Z.L.; Synthesis of biodiesel from soybean oil by coupling catalysis with subcritical methanol; Energy Conversion and Management, 2008, 49, p 3512–3516.

8. RESPONSIBILITY NOTICE

The authors are the only responsible for the printed material included in this paper.